Investigation of SLIM Dynamic Models Based on Vector Control for Railway Applications

Seyed Saeed Fazel*[1] ,Mojtaba Khorshidi[2], Mehdi Niakinezhad[3]

[1]Assistant professor, School of Railway Engineering, Iran University of Science and Technology
[2]MSc Student, School of Railway Engineering, Iran University of Science and Technology
[3]MSc Student, School of Railway Engineering, Iran University of Science and Technology

Received: 01.11.2014 *Accepted: 27.05.2015*

Abstract:
Although, Single-Sided Linear Induction Motor (SLIM) utilization has increased in railway applications due to their numerous advantages in comparison to Rotational Induction Motors (RIM), there are some sophistication in their mathematical models and electrical drive. This paper focuses on the problems of SLIM modeling, with assuming end-effect on the basis of Field Oriented Control (FOC) as a drive control method. To do so, two dynamic models of SLIM are described and investigated. To evaluate their technical characteristics (i.e., thrust, torque, current, and speed) and also motor performance, a comparison is realized for synchronous and stationary reference frames in both dynamic models. Further, the disparities of these two dynamic models and FOC operation in the two reference frames are discussed. Finally, the validity of the control method accuracy is verified for each model by simulation results.

Keywords: *electrical railway, linear induction motor, dynamic model, field oriented control*

* Corresponding Author

1. Introduction

The use of linear motor for railway traction idea is not new. In 1905, a system of 'tangential traction' was patented in Belgium, in which primary windings were to be fitted to polar projections on the track at 40 ft. intervals (Laithwaite and Barwel, 1964). Thereafter, this idea has been applied for high speed transportation systems in 1970's by many countries like Germany, USA, UK, Canada and Japan. Nowadays more than 20 transportation systems utilize Linear Motors (LM) around the world (Xu et al., 2012).

LM can be classified into two main types; Linear Induction Motor (LIM) and Linear Synchronous Motor (LSM). LIMs can be also categorized in Single-sided Linear Induction Motor (SLIM) and Double-sided Linear Induction Motor (DLIM) types (Figure 1).

Utilization of SLIM drives is improving in railway industry, due to (1) excellent acceleration and deceleration, (2) lower construction cost due to the small tunnel cross-section and flexible line choice (travel through sharp curves) which is particularly favorable for subway systems (Xu et al., 2012; Krause et al., 2013; Xu et al., 2010; Yaohua and Nengqiang, 2007) (3) capability of climbing steep gradients, (4) direct propulsive thrust, independent of the friction between the wheels and rail, and can safely be operated, even in rainy or snowy weather (Xu et al., 2012; Liu et al., 2006; Fujii et al., 2002; Fujii et al., 2003) (5) quiet and smooth running (no mechanical couplings), and (6) lower noise and less maintenance without a gear box because of the non-adherent driving. Hence, the linear electric railway system has been already used in all over the world and continuously being extended as an attractive mode of transportation in large cities (Shiri and Shoulaie, 2012).

This paper focuses on SLIMs due to their excellent applications in electric railways (Figure 2). Since primary and secondary of SLIMs have finite length, flux conditions in start and end edges of the shorter element will change due to sudden variation in rotor position. So, this will cause a considerable effect on dynamic and static performances of machine conditions, especially in higher speeds. In other words, if stator moves on the secondary surface, a magnetic field will be appeared at the beginning of stator. Also, the magnetic field at the end of the stator will be eliminated, gradually. These flux variations produce magnetic field in the secondary surface and beneath edges of stator which deviates the actual net flux distribution in the air gap. This phenomenon is known as end-effect which is reported in (Duncan, 1983; Kang and Nam, 2005; Da Silva et al., 2003; Liu et al., 2006). The end-effect compensation methods are mentioned in several papers such as (Fujii et al., 2002; Fujii et al., 2003).

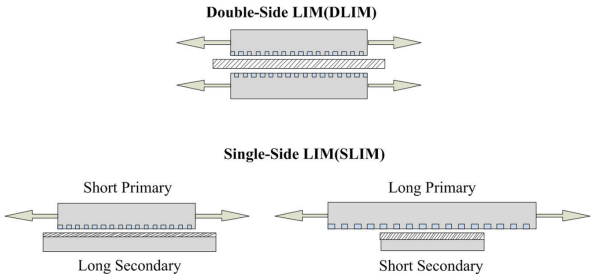

Figure 1. Single-sided and double-sided LIMs

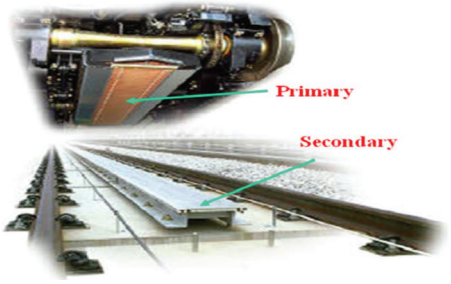

Figure 2.Application of SLIM in electric railway

2. Dynamic models of SLIM

There are two commonly used dynamic models which are equally valid for the analysis of dynamic performance of the SLIMs. In what follows, the two models and their relationships are presented in d-q reference frames (Krause et al., 2013).

A. Model A

The first dynamic model is based on T-model equivalent circuit of Rotational Induction Motor (RIM) assuming the end-effect which was first introduced by Duncan (Duncan, 1983). He derived useful function expression *f(Q)* according to secondary eddy current average value applying an energy conversion balance theorem. He indicated that the end-effect only affected on the *d*-axis equivalent circuit of SLIMs while the *q*-axis equivalent circuit is equal to RIM (Figure 3). The air-gap flux linkage varia-

tion in this model from the entrance end to the exit end, affected the SLIM performances as well as structure parameters (i.e. operating speed, secondary resistance and mutual inductance) (Xu *et al*., 2010).

This model is generally composed of the primary and secondary voltage equations and the linkage fluxes in *d-q* coordinate as follows:

$$V_{qx}=R_x i_{qx}+R_x f(Q)(i_{qx}+i_{qy})+P\lambda_{qx}-\omega\lambda_{dx} \quad (1)$$

$$V_{qy}=R_y i_{qy}+R_y f(Q)(i_{qx}+i_{qy})+P\lambda_{qy}+(\omega-\omega_y)\lambda_{dy} \quad (2)$$

$$V_{dx}=R_x i_{dy}+P\lambda_{dx}-\omega\lambda_{qx} \quad (3)$$

$$V_{dy}=R_y i_{dy}+(\omega-\omega_y)\lambda_{qy}+P\lambda_{dy} \quad (4)$$

$$\lambda_{dx} = L_{lx} i_{dx} + L_m (i_{dx} + i_{dy}) \quad (5)$$

$$\lambda_{qx} = L_{lx} i_{qx} + L_m (1 - f(Q))(i_{qx} + i_{qy}) \quad (6)$$

$$\lambda_{dy} = L_{ly} i_{dy} + L_m (i_{dx} + i_{dy}) \quad (7)$$

$$\lambda_{qy} = L_{ly} i_{qy} + L_m (1 - f(Q))(i_{qx} + i_{qy}) \quad (8)$$

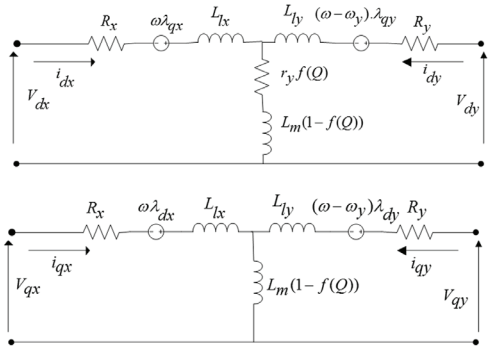

Figure 3.The d-q equivalent circuits of SLIM for model A

B. **Model B**

The second dynamic model of SLIMs assuming the end-effect has been introduced in (Kang and Nam, 2005).

It is based on symmetrical *d-q* axis models considering the mutual inductance influenced by the eddy current, regardless of the secondary resistance effect (Figure 4). The eddy current loss which is modeled with R_{eddy} does not make a significant difference in the current behavior. Therefore, in this paper R_{eddy} is neglected and only Duncan's magnetizing inductance is considered.

All the equations in *d-q* coordinate related to model B are given by (9)-(16).

$$V_{dx} = R_x i_{dx} + P\lambda_{dx} - \omega\lambda_{qx} \quad (9)$$

$$V_{qx}=R_x i_{qx}+P\lambda_{qx}-\omega\lambda_{dx} \quad (10)$$

$$V_{dy}=R_y i_{dy}+P\lambda_{dy}+(\omega-\omega_y)\lambda_{qy} \quad (11)$$

$$V_{qy}=R_y i_{qy}+P\lambda_{qy}+(\omega-\omega_y)\lambda_{dy} \quad (12)$$

$$\lambda_{dx} = L_{lx} i_{dx} + L_m (1 - f(Q))(i_{dx} + i_{dy}) \quad (13)$$

$$\lambda_{qx} = L_{lx} i_{qx} + L_m (1 - f(Q))(i_{qx} + i_{qy}) \quad (14)$$

$$\lambda_{dy} = L_{ly} i_{dy} + L_m (1 - f(Q))(i_{dx} + i_{dy}) \quad (15)$$

$$\lambda_{qy} = L_{ly} i_{qy} + L_m (1 - f(Q))(i_{qx} + i_{qy}) \quad (16)$$

The *d-q* equivalent circuits of both dynamic models are depicted in Figures 3 and 4. The differences between two models are in traversal branch taking into end-effect and eddy current. In the above equations Q and $f(Q)$ are defined using the same equations (17), (18) for both models.

$$Q = \frac{lR_y}{(L_{lx} + L_m)v} \quad (17)$$

$$f(Q) = \frac{1 - e^{-Q}}{Q} \quad (18)$$

Where Q is a factor related to the primary length which quantifies the end-effect as a function of speed (Yaohua and Nengqiang, 2007). The thrust force and linear speed for both models are described as:

$$F_e = \frac{3n_P\pi}{4\tau}(\lambda_{dx} i_{qx} - \lambda_{qx} i_{dx}) = M\frac{dv}{dt} + Dv + F_L \quad (19)$$

$$v = \frac{\omega_y \tau}{\pi} \quad (20)$$

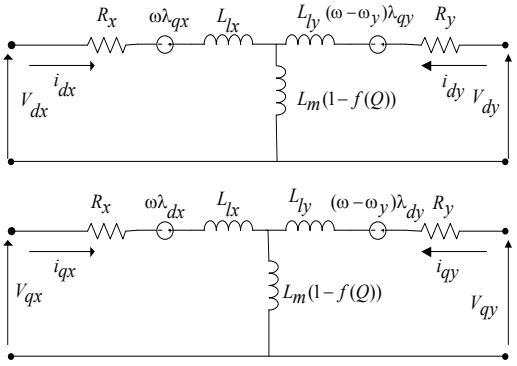

Figure 4. The d-q equivalent circuits of SLIM for model B

3. Field oriented control for SLIM

Flux Oriented Control (FOC) is a well-known advanced control scheme. It has an excellent dynamic performance

mainly due to decoupled control of stator magnetic field and electromagnetic torque as the same of Direct Current (DC) motor drive. The aim of FOC is maintaining constant d-axis secondary flux and making zero the *q*-axis secondary flux. This section focuses on FOC scheme for SLIM drives, which is similar to RIM (Da Silva *et al*., 2003). It uses the rotor FOC scheme due to its simplicity. In this paper for the sake of better performance, high reliability and simplicity Indirect Field Oriented Control (IFOC) method is selected. A general block diagram of a SLIM drive with IFOC is shown in Figure 5. There are three closed loops including linear speed, *d*-axis flux and *q*-axis current loops which are modified by three PI controllers. The outputs of PI controllers make command voltages in synchronous reference frames as inputs of dq/abc transformer block. The final abc voltage commands are utilized for switching of inverter.The slip angular frequency can be calculated by equations (21) and (22) applying $\lambda_{qy}=0, \lambda_{dy}=\lambda_d$ to both models respectively. Rotor flux angle θ_e is determined by equation (23).

$$\omega_{sl}=\frac{L_m R_y[1-f(Q)]}{[L_y-L_m f(Q)]\lambda_{dy}} i_{qx} \quad (21)$$

$$\omega_{sl}=\frac{L_m R_y}{L_y \lambda_{dy}} i_{qx} \quad (22)$$

$$\theta_e=\int \omega_{sl}dt+\int \omega_r dt \quad (23)$$

The secondary linkage fluxes in *d*-axis λ_{dy} are described as follows for both models, respectively:

$$\lambda_{dy}=\frac{[L_m-L_y f(Q)]R_y}{[L_m-L_y f(Q)]P+R_y[1+f(Q)]} i_{dx} \quad (24)$$

$$\lambda_{dy}=\frac{L_m R_y[1-f(Q)]}{R_y+[L_y-L_m f(Q)]P} i_{dx} \quad (25)$$

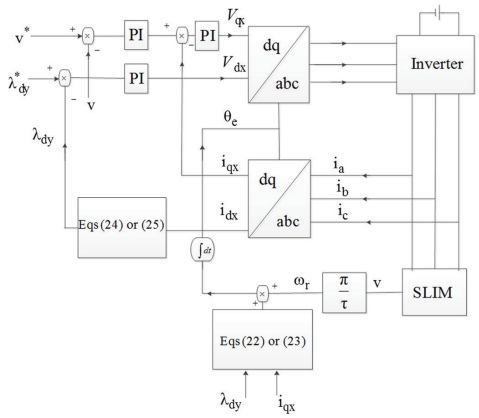

Figure 5. The d-q equivalent circuits of SLIM for model B

Simulation results

In this section dynamic characteristics of both SLIMs are investigate under synchronous and stationary reference frames considering motor parameters (Table I).

Figure 6 demonstrates linear speed of both models in synchronous and stationary reference frames during free acceleration (no-load). Although the speed will remain unchanged in model B for both reference frames (Figure 6b and Figure 6d), but it shows a different behavior in model A (Figure 6a and Figure 6c). The modeling of the end-effect in both dynamic models is the main reason for this difference. In other word, the first model has an asymmetrical nature compared with the second model.

It is obvious that the settling time of speed in synchronous reference frame is about 170 sec. (Figure 6a) in comparison with 2 sec. in stationary reference frame in model A (Figure 6c).

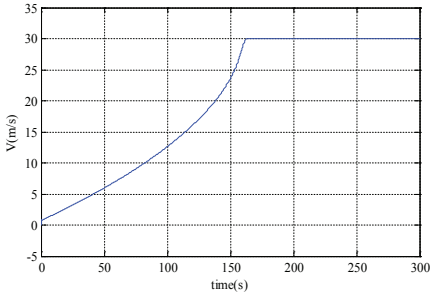

(a)

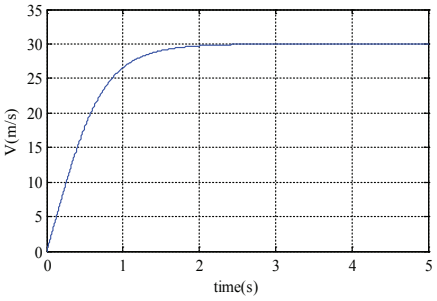

(b)

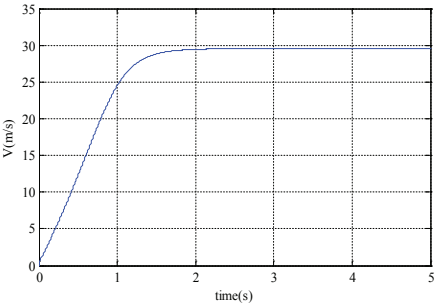

(c)

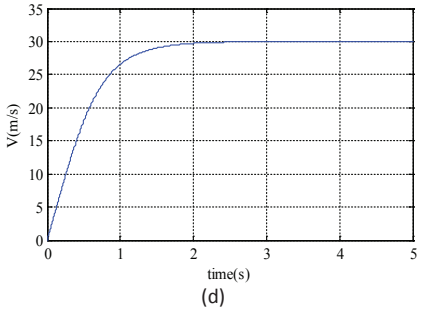

(d)

Figure 6.Speed response in synchronous reference frame :a) model A, b) model B Speed response in stationary reference frame c) model A, d) model B

Thrust force waveforms during free acceleration (no-load) in synchronous and stationary reference frames of model A and B are shown in Figure 7. End-effect influences transient response of the thrust waveforms for synchronous reference frame in model A (Figure 7a) in comparison with the other ones (Figures 7b, 7c, and 7d). Also it causes an oscillation around zero (peak to peak 120 N) in the steady state response of stationary reference frame in model A (Figure 7c).Figure 8 indicates only the *q*-axis current waveforms of model A and B in both synchronous and stationary reference frames during free acceleration (no-load). As expected, Figures 8a and 8b have the dc current waveforms in synchronous reference frame of model A and B respectively, while Figures 8c and 8d have the sinusoidal current waveforms in stationary reference frame. As it is clear the synchronous reference frame current waveform of model A reaches the final value after 170 sec. due to slow speed response. It is obvious that the values of the current amplitude in model A (-105 Amp. and 216 Amp. peak to peak for synchronous and stationary reference frames respectively) are greater than the values in model B (-91 Amp. and 182 Amp. peak to peak for synchronous and stationary reference frames respectively) due to R_{eddy} loss in equivalent circuit in both reference frames of model A.

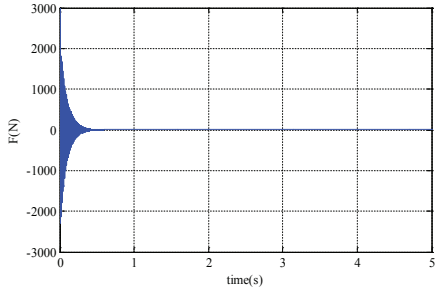

(a)

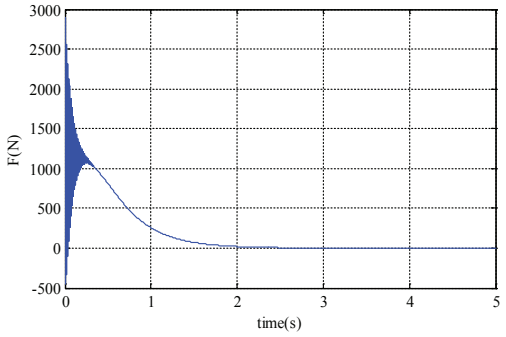

(b)

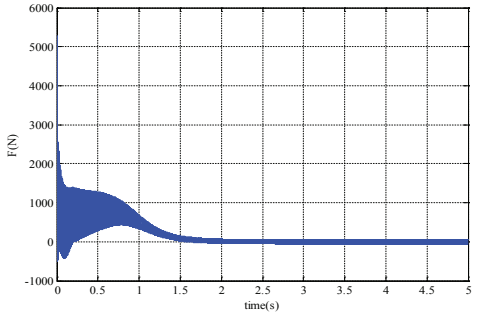

(c)

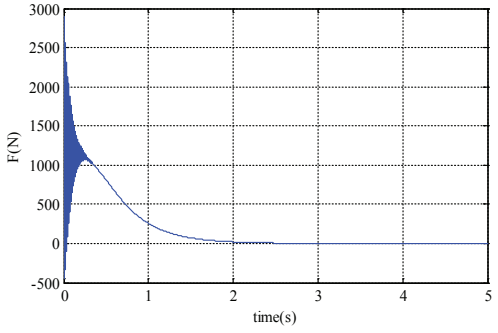

(d)

Figure 7.Thrust force waveforms in synchronous reference frame :a) model A, b) model B Thrust force waveforms in stationary reference frame c) model A, d) model B

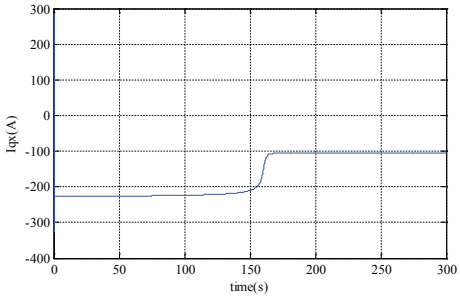

(a)

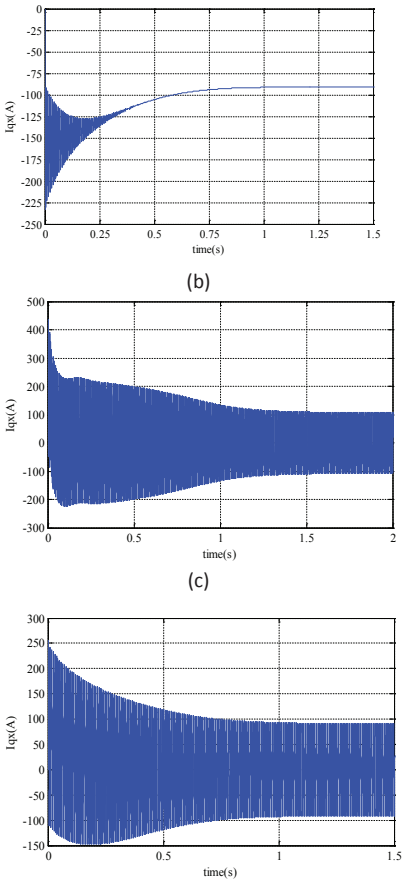

Figure 8.Current waveforms in synchronous reference frame :a) model A, b) model B Current waveforms in stationary reference frame c) model A, d) model B

All previous simulations are done under free acceleration conditions regardless of the control scheme. In this section operational analysis of the two models (A and B) by applying the IFOC method in stationary reference frame are presented.The linear speed and primary phase current are shown in figure 9. To investigate the dynamic behavior of SLIM using IFOC, the initially reference of linear speed command is set to 6 m/s. The linear speed changes after 1 sec. from 6 m/s to 20 m/s. The results indicate further fluctuations at start time (t=1 sec.) as well as over-shoot of about 12% at command time (t=6 sec.) in model A compared to model B (figure 9a). Therefore, it is expected that the linear speed of model A has intensive oscillations due to inductance property of motor. Also this drastic fluctuation of model A imposes large amount of voltage drop in primary side inductances which represents the inaccuracy of the modeling in model A (figure 9b). This value is not acceptable in case of the typical SLIMs.

TABLE 1 PARAMETERS OF SLIM

Parameter	Value	Parameter	Value
$R_x(\Omega)$	0.0488	$M(kg)$	29.34
$R_y(\Omega)$	0.802	$l(m)$	0.412
$L_{lx}(H)$ 0.0014		$\tau(m)$	0.102
$L_{ly}(H)$	0	n_p	4
$L_m(H)$	0.003	$f(Hz)$	146.5

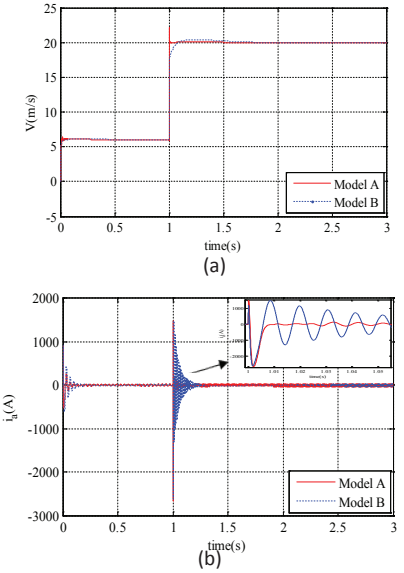

Figure 9.a) Linear speed and b) Current waveforms based on IFOC as control method

5. Conclusions:

The dynamic models of SLIM assuming end-effect were investigated and compared. To examine the effect of each dynamic model on the technical specifications, both models were compared in two different reference frames (synchronous and stationary). The simulation results showed that the speed and thrust force waveforms remained unchanged for model B in both synchronous and stationary reference frames. On the contrary, this signals represented the different behavior in model A for two different reference frames (the settling time of linear speed in synchronous reference frame is approximately 85

times greater than the stationary reference frame), which represents the inaccuracy of model A due to the asymmetrical nature in mathematical equations compared with the model B.

The values of the current amplitudes in model A were 15% and 18% higher than model B in synchronous and stationary reference frames respectively due to R_{eddy} loss in equivalent circuit in of model A.

In the last section operational analysis of two models by applying the IFOC method in stationary reference frame were presented. The results showed further fluctuations at start time as well as over-shoot of about 12% at command time in model A compared to model B. Therefore, it is expected that the linear speed of model A had intensive oscillations due to inductance property of motor. Also this drastic fluctuation of model A imposed large amount of voltage drop in primary side inductances which represents the inaccuracy of the modeling in model A. This value is not acceptable in case of the typical SLIMs.

6. References

- Laithwaite ER and Barwell FT. (1964) Linear induction motors for high-speed railways. *Electronics & Power* **10(4)**: 100-103.

- Xu W, Sun G, Wen G, et al. (2012) Equivalent circuit derivation and performance analysis of a single-sided linear induction motor based on the winding function theory*., IEEE Transactions on Vehicular Technology* **61(4)**: 1515-1525.

- Duncan J. (1983) Linear induction motor-equivalent-circuit model. *IEE Proceedings B (Electric Power Applications). IET* **130(1)**: 51-57.

- Kang G and Nam K. (2005) Field-oriented control scheme for linear induction motor with the end effect. *Electric Power Applications, IEE Proceedings-. IET*, **152(6)**: 1565-1572.

- Da Silva EF, Dos Santos EB, Machado PCM, *et al*. (2003) Vector control for linear induction motor*., 2003 IEEE International Conference on Industrial Technolog.*, pp. 518-523.

- Liu J, Lin F, Yang Z et al. (2006) Field oriented control of linear induction motor considering attraction force & end-effects. *Power Electronics and Motion Control Conference*,pp. 1-5.

- Fujii N, Kayasuga T and Hoshi T. (2002) Simple end effect compensator for linear induction motor., *IEEE Transactions on Magnetics* **38(5)**: 3270-3272.

- Fujii N, Harada T, Sakamoto Y *et al*. (2003) A compensation method for the end effect of a linear induction motor. *Electrical Engineering in Japan* **143(3)**: 58-67.

- Krause PC, Wasynczuk O, Sudhoff SD, *et al*. (2013) Analysis of electric machinery and drive systems: *John Wiley & Sons*.

- Xu W, Zhu JG, Zhang Y *et al*. (2010) Equivalent circuits for single-sided linear induction motors., *IEEE Transactions on Industry Applications* **46(6)**: 2410-2423.

- Yaohua L and Nengqiang J. (2007) A New Parameter Measurement Scheme for Single Linear Induction Motors [J]. *Transactions of China Electrotechnical Society* **22(4)**: 56-61.

-Shiri A and Shoulaie A. (2012) Design optimization and analysis of single-sided linear induction motor, considering all phenomena., *IEEE Transactions on Energy Conversion* **27(2)**: 516-525.

Nomenclature

x, y	Primary and secondary subscript respectively
q, d	Subscript related to q-, and d-axis
L_y , L_x	Primary and secondary inductances
L_{ly} , L_{lx}	Primary and secondary leakage inductances
V_{dx}, V_{qx}	Primary voltages
V_{dy}, V_{qy}	Secondary voltages
i_{dx}, i_{qx}	Primary electrical currents

i_{dy}, i_{qy}	Secondary electrical currents
R_y , R_x	Primary and secondary resistances
ω_r	Rotor angular frequency
ω	Arbitrary reference-frame speed
$\lambda_{dx}, \lambda_{qx}$	Primary flux
$\lambda_{dy}, \lambda_{qy}$	Secondary flux
n_P	Pole number
l	Primary length
τ	Pole pitch
ω_{sl}	Slip angular frequency
M	Mass of moving element
D	Viscous friction
F_L	External force
P	Differential operator
v	Linear speed